

Spectral similarity fault enhancement

Dustin T. Dewett¹ and Alissa A. Henza¹

Abstract

Fault interpretation in seismic data is a critical task that must be completed to thoroughly understand the structural history of the subsurface. The development of similarity-based attributes has allowed geoscientists to effectively filter a seismic data set to highlight discontinuities that are often associated with fault systems. Furthermore, there are numerous workflows that provide, to varying degrees, the ability to enhance this seismic attribute family. We have developed a new method, spectral similarity, to improve the similarity enhancement by integrating spectral decomposition, swarm intelligence, magnitude filtering, and orientated smoothing. In addition, the spectral similarity method has the ability to take any seismic attribute (e.g., similarity, curvature, total energy, coherent energy gradient, reflector rotation, etc.), combine it with the benefits of spectral decomposition, and create an accurate enhancement to similarity attributes. The final result is an increase in the quality of the similarity enhancement over previously used methods, and it can be computed entirely in commercial software packages. Specifically, the spectral similarity method provides a more realistic fault dip, reduction of noise, and removal of the discontinuous “stair-step” pattern common to similarity volumes.

Introduction

The application of seismic attributes to fault identification originates from work by Bahorich and Farmer (1995) through the development of the coherence algorithm (crosscorrelation of adjacent seismic traces), which resulted in great efficiency gains by seismic interpreters. However, the early coherence attribute performed poorly in high-noise data sets. The second-generation similarity algorithm, based on multitrace semblance, has less noise sensitivity (Marfurt et al., 1998). A major drawback to these methods is the sensitivity to amplitude discontinuities. Garshtenkorn and Marfurt (1999) propose a third-generation similarity algorithm computed through the calculation of the eigenvalues of a covariance matrix over a window of seismic data, which removed the amplitude sensitivity while increasing and localizing the fault response on the seismic data. Improvements to dip estimation quickly followed through the development of the dip scan method, which provides superior accuracy and precision to dip estimates in seismic data (Marfurt, 2006). Numerous edge detection algorithms followed including the introduction of the Sobel filter to seismic data by Aqrabi and Boe (2011).

Soon after the development of edge detection algorithms, came the concept of computer-based fault interpretation. In 2001, similarity attributes were used for computer-based fault extraction, and it was quickly identified that “conditioning” or enhancement of the

similarity attribute would be a major and critical step (Randen et al., 2001). The idea of similarity enhancement directly led to the application of ant colony optimization to fault extraction causing a major step forward for the industry (Pedersen et al., 2002). Nonetheless, Aqrabi and Boe (2011) make the very specific point several years later, “[a]utomatic fault detection and extraction is still considered to be a major challenge for the industry.” In an attempt to address this same problem, Dorn et al. (2012) develop the fault-enhanced attribute (also called AFE). Although independent of the swarm intelligence methods proposed by Pedersen et al. (2002), it was an equal step forward in thinking for the industry.

One of the key tasks in seismic interpretation is the identification of faults, and the efficiency gains that are possible through computer-based fault extraction are enormous. Unfortunately, the similarity attributes described earlier are known for poor vertical resolution and are more often used through horizontal slices or horizon extraction based interpretation. This results in poor computer extractions. The major goal of similarity enhancement is to improve the vertical axis response of the similarity volume and the computer-based fault interpretations. We propose a new method for enhancing the similarity volume, spectral similarity, which produces a volume that increases the efficiency of fault interpretation several times over traditional

¹BHP Billiton, Petroleum, Houston, Texas, USA. E-mail: dustin.dewett@bhpbilliton.com; ahenza@gmail.com.

Manuscript received by the Editor 16 July 2015; revised manuscript received 10 October 2015; published online 24 February 2016. This paper appears in *Interpretation*, Vol. 4, No. 1 (February 2016); p. SB149–SB159, 12 FIGS.

<http://dx.doi.org/10.1190/INT-2015-0114.1>. © 2016 Society of Exploration Geophysicists and American Association of Petroleum Geologists. All rights reserved.

human-based fault interpretation and computer-based fault extraction techniques (Figure 1).

Definitions

Key terms for this paper include the following:

- Similarity is a family of edge detection attributes that include coherence, variance, the Sobel filter, or similar algorithms.
- Swarm intelligence is a family of algorithms that use decentralized self-organization to perform a task (examples include particle swarm optimization, ant colony optimization, or differential evolution).
- Machine learning is a subdiscipline of computer science that consists of algorithms that can learn from and make predictions on data (examples include artificial neural networks, self-organized maps, and k -means clustering).

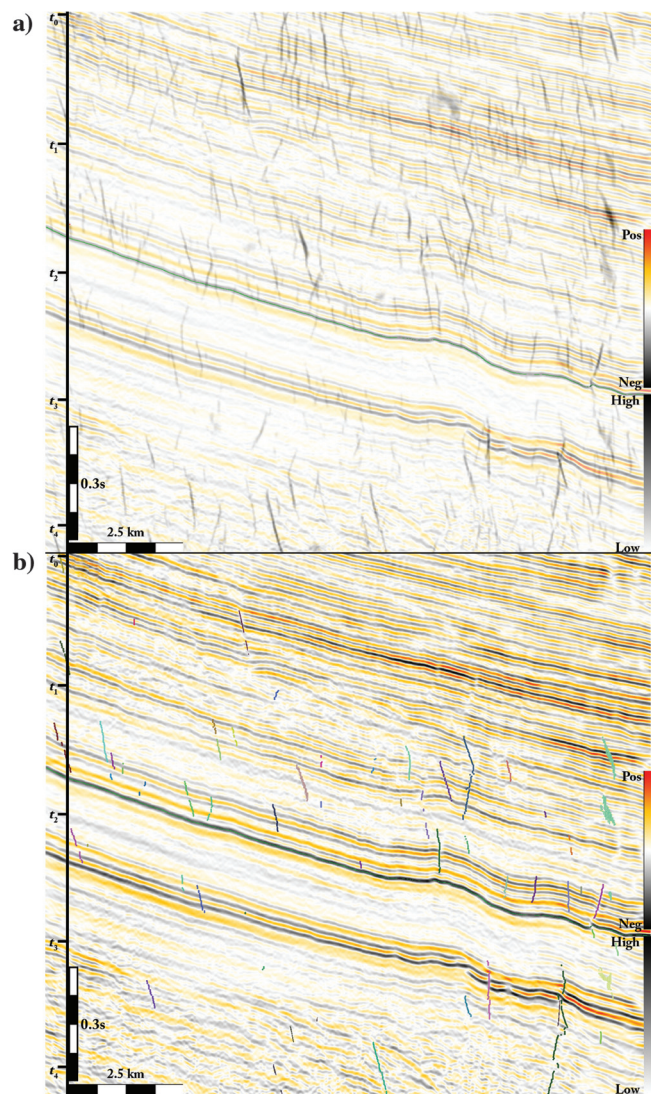


Figure 1. Vertical section of the (a) spectral similarity corendered with seismic amplitude and (b) faults extracted using computer-based fault interpretation derived from the spectral similarity corendered with seismic amplitude.

- Spectral similarity refers to the workflow described in this paper for similarity enhancement.

Motivation

Above, we mention two major steps forward in the enhancement of similarity volumes by Pedersen et al. (2002) and Dorn et al. (2012). Both of these approaches provide a unique look at fault enhancement, which produce very different results. As we will discuss, spectral similarity draws from these ideas with the aim of improving upon them. Both of these methods perform well in many situations. However, we will focus upon their respective weaknesses because they perform poorly in similar situations and our goal is to improve upon those specific weaknesses.

The Pedersen et al. (2002) similarity enhancement uses the ant colony optimization technique (a swarm intelligence algorithm) to connect discontinuous similarity events and remove the common stair-step anomaly seen in many similarity-based attributes. This algorithm excels at fault connectivity and the retention of appropriate fault dip. However, this technique is very sensitive to noise and is not generally appropriate for any but the largest faults (Figure 2a). Aqrabi and Boe (2011) attempt to improve the results of this swarm intelligence technique by improving the underlying similarity attribute by changing from a semblance-based to a Sobel filter-based attribute. Although this improved the results significantly, the inherent sensitivity of ant colony techniques (and likely all swarm intelligence algorithms) to noise is significant.

The Dorn et al. (2012) AFE is a seismic attribute centered on user-driven filtering of the similarity magnitude combined with an orientated smoothing parameter (Figure 2b). This technique excels in the detection of large faults, and, owing to the smoothing parameters, provides excellent fault connectivity in those situations. However, the technique suffers from poor performance in the presence of small- to medium-sized faults and lacks a method of interpolation to increase fault connectivity.

The vast majority of similarity enhancement techniques (including those mentioned above) commonly suffer from three major classes of detection issues (although not every method suffers from all classes). The first is an abundance of near-vertical similarity response — an effect likely related to either the algorithm or the underlying similarity attribute (see the solid rectangles in Figure 2). The second is the inherited stair-step anomaly that is a common effect seen in the underlying similarity volume (see the dotted rectangles in Figure 2). Third, many faults are realistically oriented, but they appear broken and discontinuous (see the dashed rectangles in Figure 2). It is these three classes of similarity enhancement problems that we are attempting to improve through our proposed spectral similarity attribute workflow.

Spectral similarity

As shown in Figure 2c, spectral similarity improves upon all three classes of problems discussed above. Spectral similarity results in fault dips that are in general agreement with the expectations by area experts and structural geologists, the removal of stair-step errors, and greatly improved fault connectivity. In addition, the range of values (represented by the change in fault colors from light gray to black) implies a confidence or probability in the volume. In practice, this attribute, when used with a computer-based fault interpretation technique, can be further filtered by this confidence to yield very realistic fault surfaces.

As discussed below, we begin with spectral decomposition; therefore, each attribute parameter and filter is customized to a given frequency band. Our technique is, therefore, highly adaptable to a range of data sets. For example, when computing a similarity volume, one key input is the vertical window height, which ideally is a function of the dominant wavelength of the interval of interest. This results in suboptimal parametrization in all areas with different dominant wavelengths (which can vary laterally and vertically). However, in a spectral volume, the optimal window height represents the dominant wavelength of the entire volume. If a data set has

significant frequency contrasts between the shallow and deep section (e.g., subsalt Gulf of Mexico), one can create a spectral similarity with frequency components for a shallow section that are drastically different than for the deeper section. Another beneficial feature of spectral similarity is the ability to incorporate any attribute type into the process (e.g., dip magnitude, curvature, reflector rotation, etc.). It is precisely this customizable feature that allows spectral similarity to excel in every data set and basin in which it was applied (regardless of differences in geology).

Workflow description

The general form of our workflow is independent of specific techniques or approaches (Figure 3). The spectral similarity workflow provides a great deal of customization based on individual preferences, data quality, and time constraints. Therefore, it is not possible to define the exact workflow for any given data set or project, but the optimal customized algorithm is quickly identified when constraints (data or time) are applied.

We begin with a seismic data set that is filtered, as needed, for attribute analysis. Then we follow with spectral decomposition (e.g., short-time Fourier transform, continuous wavelet transform [CWT], matching

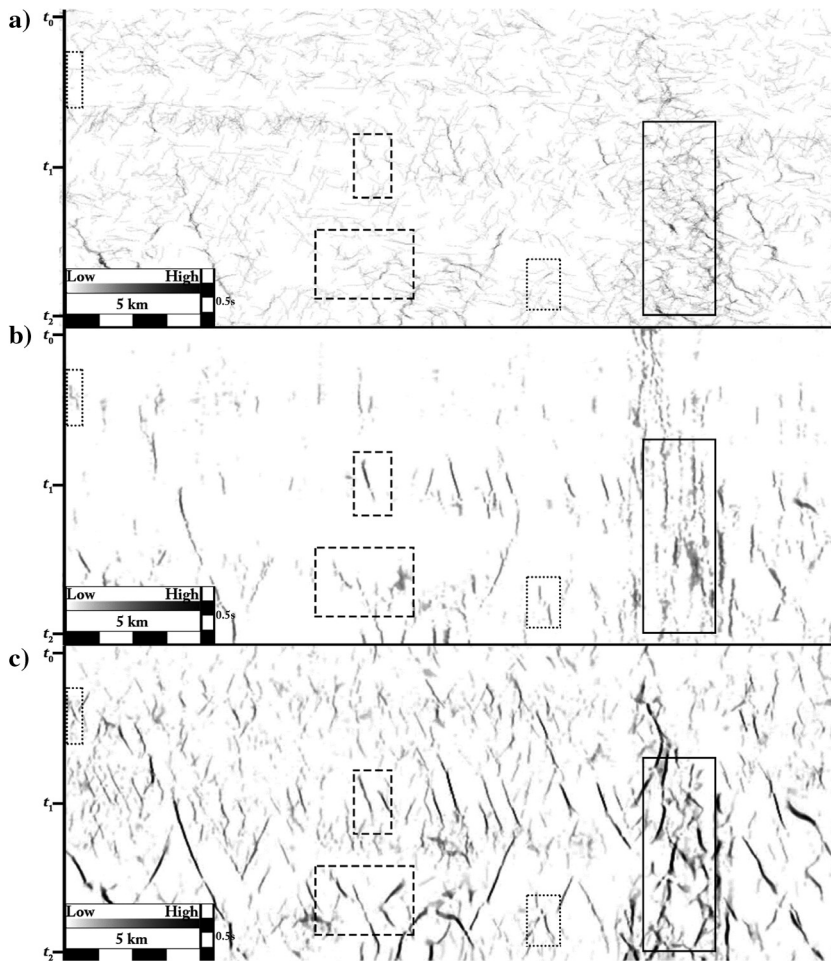


Figure 2. Composite vertical section image of the same crossline using various edge enhancement calculations. (a) Swarm intelligence method proposed by Pederson et al. (2002). (b) Strike- and dip-based enhancement proposed by Dorn et al. (2012). (c) Spectral similarity proposed in this paper. Three different classes of anomalies are highlighted based on the characteristics of the Pederson et al. and Dorn et al. style enhancements: (1) solid rectangles indicate areas of poorly imaged faults, (2) dotted rectangles indicate areas in which are moderately well imaged, and (3) dashed rectangles indicate well-imaged faults improved in the spectral similarity attribute.

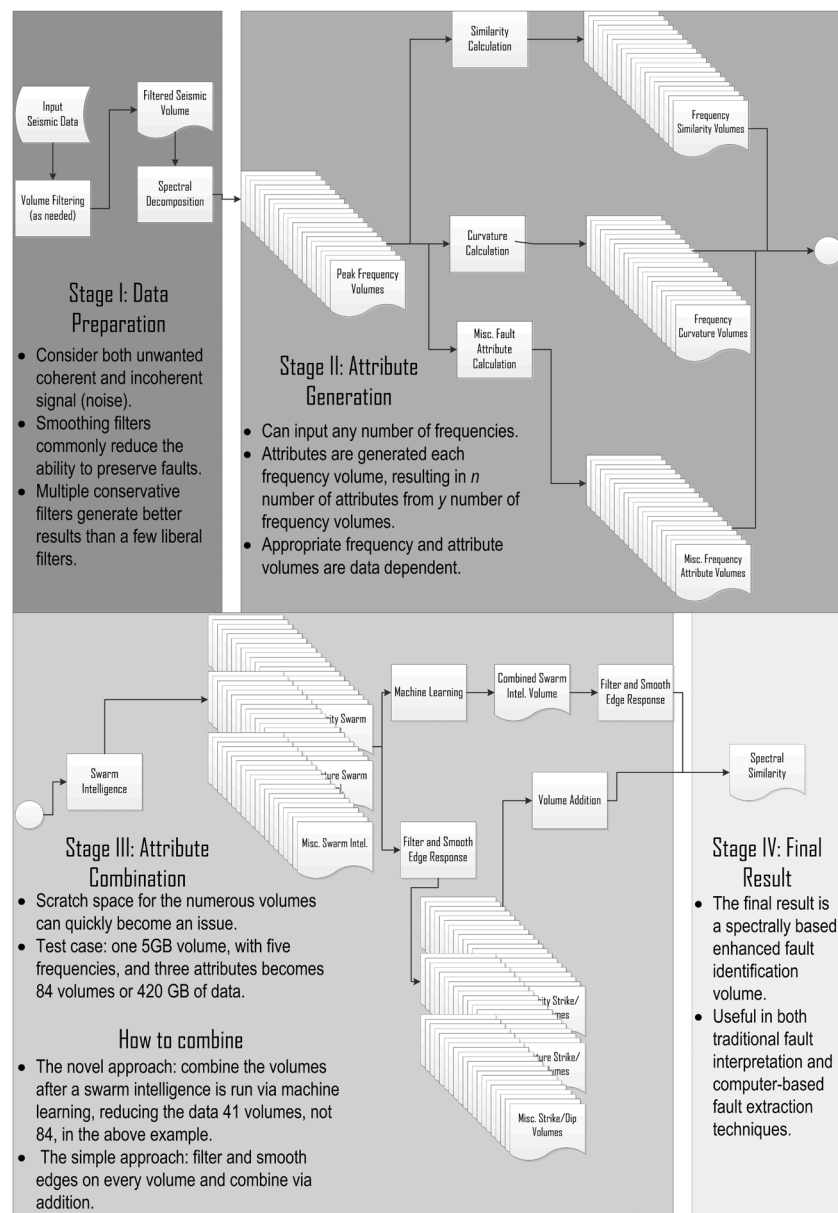
pursuit, crosscorrelation, or constrained least-squares spectral analysis; Figure 3a). These peak-frequency volumes (i.e., spectral voice or similar) are used to compute the seismic attributes (Figure 3b). Our experience indicates that higher frequencies (greater than 30 Hz) are more beneficial than are low frequencies (less than 15 Hz), but this is data dependent. We commonly use geometric attributes calculated from these data; however, this workflow can be adopted to use other derivative volumes (e.g., the spectral phase) directly by skipping the attribute generation step and applying the swarm intelligence-based attribute to these volumes directly. Numerous frequency-based attributes are used as input to swarm intelligence for lineament connection and interpolation between discontinuous events (Figure 3c). In the final portion of the workflow, we use each of these swarm intelligence volumes as an input

into edge-filtering and smoothing operations. We then combine each of these spectral fault-enhanced volumes through addition, resulting in a similarity that has been enhanced through the inclusion of spectral decomposition (Figure 3d). An alternative method to combine the various volumes is through a machine-learning algorithm (in our tests, we used a self-organized map), a technique adapted from Basir et al. (2013). This adds additional computation time, but it significantly reduces the amount of intermediate data volumes created (Figure 4 shows the results of this optional approach).

Workflow customization

It is common for individuals to have preferences and biases to particular algorithms. This is why we present the spectral similarity algorithm in generic terms. The optimum spectral decomposition or similarity method

Figure 3. The spectral similarity workflow and its four main stages of generation. The bifurcation in stage III allows for two different techniques to combine the results.



will vary depending on the data specifics. Moreover, individual biases or company policy may further constrain algorithms (e.g., if corporate policy maintains the use of only Sobel filter similarity). In addition, some algorithms and implementations take considerably longer to compute than do others. Therefore, when time constraints, personal/corporate bias, and data-dependent, goal-based constraints are applied, the ideal workflow for a given project is easily identified.

Case study no. 1: High signal to noise

The first data set chosen to illustrate our method is from central Texas, USA. In general, this area is an extensional regime, with normal faults striking approximately perpendicular to the extension direction. However, the underlying structure of the region and vertical stratigraphic variations has influenced the deformation patterns in this package, resulting in multiple fault orientation trends and detachment levels. A paleoreef

(Figure 5c) is a prominent feature along which many faults nucleate and terminate, creating a fault trend that is oblique to the regional paleostress field. In addition, early movement of the underlying salt created local variations in the stress regime that affected later faulting (Figure 5b and 5d). Owing to the local and regional paleostresses, we expect the fault patterns to be dominated by normal faults with orientations that vary laterally. The data set is of excellent quality with minimal noise. The notable exception to this is the relatively low signal-to-noise area (Figure 5a).

Customized workflow

We began with a crosscorrelation-based spectral decomposition (Gao, 2013). This type of spectral decomposition is acceptable for geometric interpretation, and the computation time is shorter than for other methods. We used three volumes at approximately 20, 37, and 43 Hz to compute a modified eigenstructure similarity

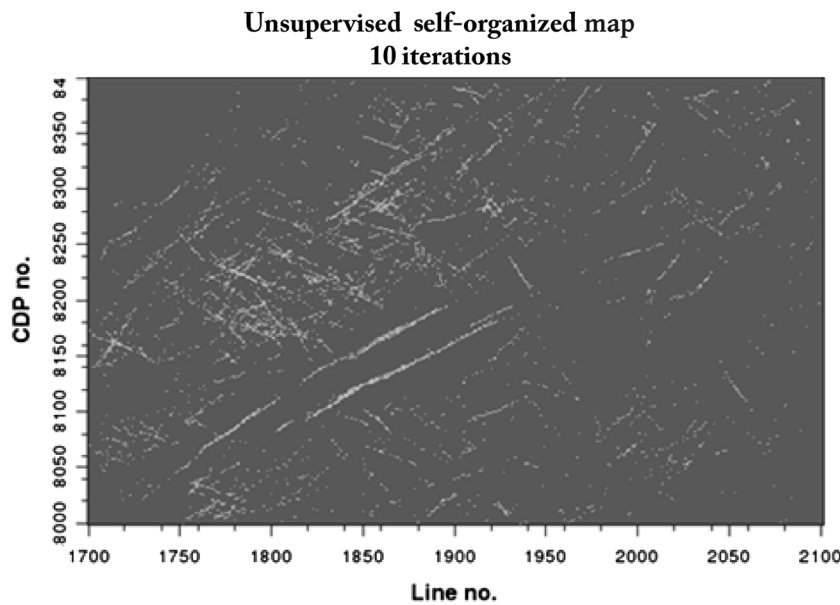


Figure 4. A time slice of a machine learning algorithm (self-organized maps) being used to combine three swarm-intelligence volumes into one prior to the filter and smoothing step.

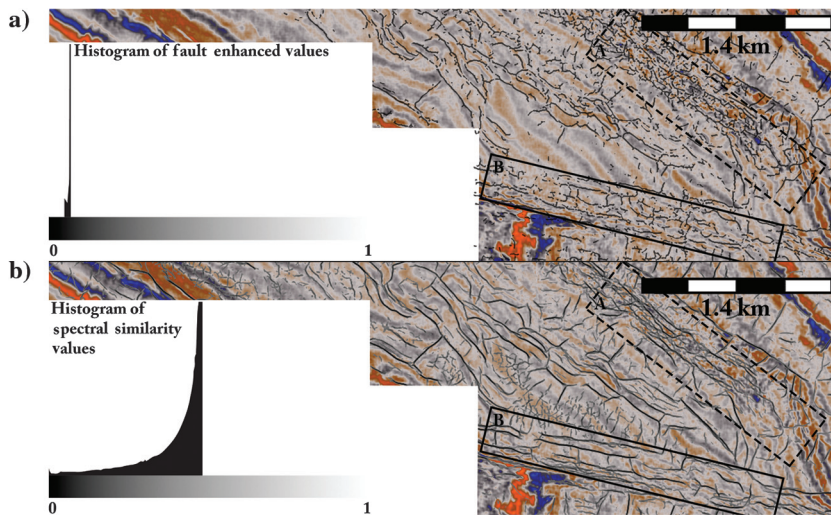


Figure 5. Time slice through the seismic amplitude volume corendered with the (a) fault-enhanced similarity and (b) the spectral similarity that illustrates the data quality and lateral variation of seismic character in the data set. The rectangles highlight areas of interest, which include (A) a low signal-to-noise zone, (B) lateral changes to geology, (C) the response to stratigraphic thinning, and (D) a high signal-to-noise zone with large faults. A histogram for each similarity enhancement is shown highlighting the range of values of those volumes.

for each spectral volume (Garshtenkorn and Marfurt, 1999). When calculating dip, we used a dip-scan method with a maximum of 30° and an increment of 2° (Marfurt, 2006). We followed with swarm intelligence described by Pedersen et al. (2002), and a magnitude-based filtering and smoothing operation (Dorn et al., 2012) on each frequency volume. Finally, we added the three frequency-based attribute volumes together. The total size of the original seismic is approximately 17 GB, and the total size of all intermediate volumes, parameter tests, software projects, duplicated data, and SEGY exports is 969 GB. Most of these data were intermediate scratch data that were not retained.

Results

To evaluate the quality of the resultant spectral similarity, we asked two dozen structural and geophysical experts (with an average of 17 years of experience, knowledge of multiple basins, and several Ph.D. holders) to compare our results to a traditional similarity

volume. The response was a preference among all geoscientists for the spectral similarity algorithm (approximately 96% favorable).

Figure 6 illustrates two fault enhancements to the similarity volume, the fault-enhanced volume (Dorn et al., 2012) and spectral similarity discussed in this paper. The quality of the enhancement varies laterally, owing to zones of relatively poor signal to noise and changes in peak frequency. The spectral similarity results in more distinct fault patterns and interactions than the fault-enhanced volume. Specifically, the spectral similarity volume (Figure 6b) performs very well in area A, where a large fault zone significantly reduces the signal-to-noise ratio (S/N). Areas B and D have significantly improved fault connectivity in the spectral similarity volume and provide an excellent guide for fault interpretation and refinement of existing fault surfaces. In addition, the increased range of values of the data yields an implied level of confidence directly from the data volume. The darker faults are more pro-

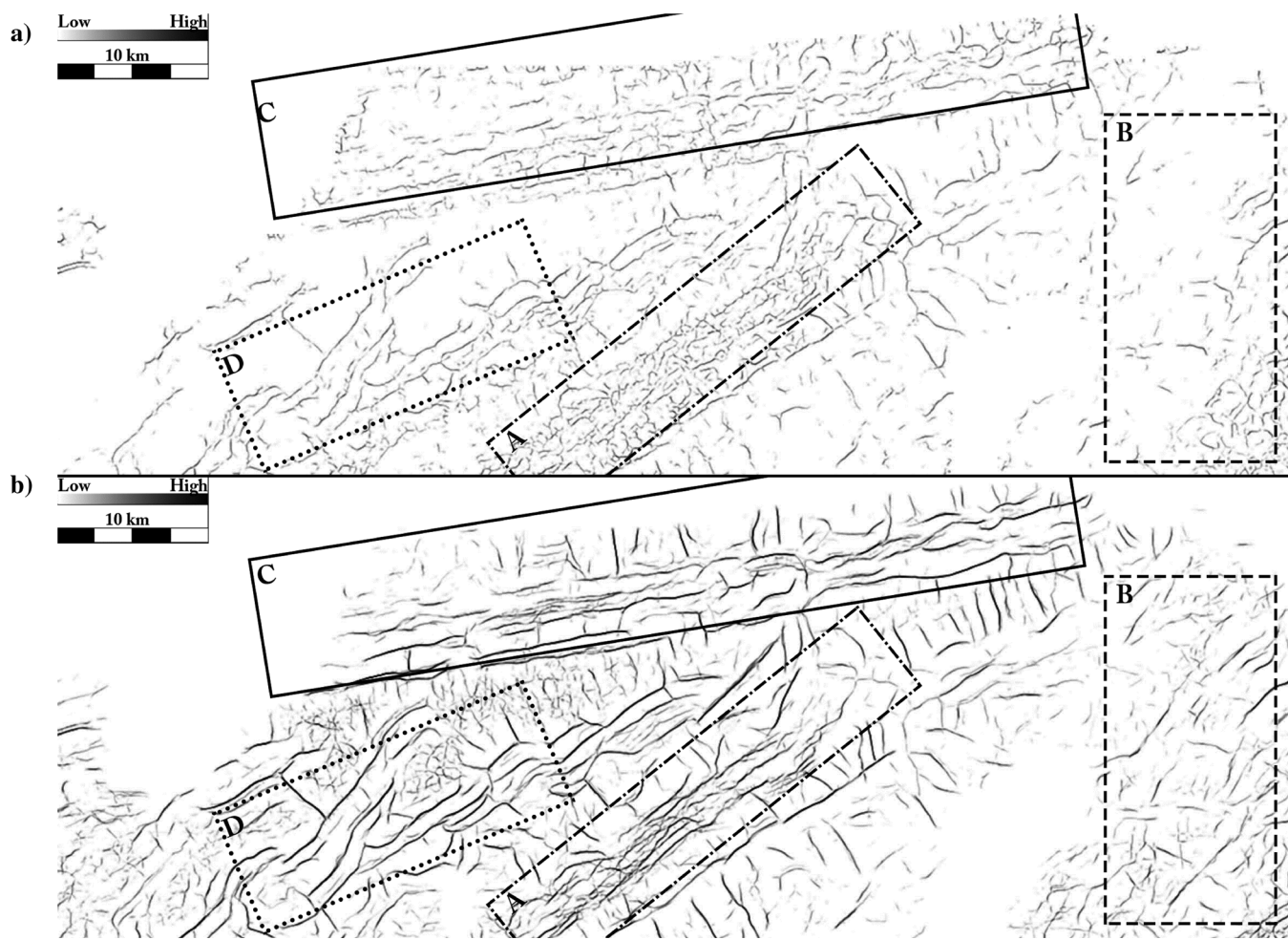


Figure 6. Time slice of the (a) fault-enhanced volume and (b) spectral similarity volume derived from the amplitude shown in Figure 5. In area A, the noise from a major fault zone makes any fault interpretation from the fault-enhanced volume difficult, whereas spectral similarity can easily interpret the major faults. The faults in the fault-enhanced volume in area B (which cuts into the overlying formation) have been filtered out. The faults in this same area in the spectral similarity are present and clear, owing to the multiple volumes that comprise the spectral similarity attribute. Similarly, areas C and D in the fault-enhanced volume lack the fault connectivity and clarity that is present in the spectral similarity.

nounced in the spectral similarity method than in the fault-enhanced method, whereas the lighter colors may be smaller faults or even an artifact (i.e., the typical double-fault expression commonly seen in time-migrated data). Differences between the fault-enhanced and the spectral similarity method are also visible in the vertical section (Figure 7a; the full supplementary figure can be accessed through the following link: [s1.mpg](#)). The fault-enhanced method commonly results in fault dips that are nearly vertical, whereas the spectral similarity method results in faults that are dipping at moderate angles (Figure 7b).

The ultimate goal of any similarity product is to aid in interpretation. Figure 8 shows the spectral similarity corendered with the seismic amplitude, illustrating

how an interpreter can use both products for manual or computer-based interpretation. Preexisting faults can also be refined by using spectral similarity for quality control. The noticeable increase in the sharpness of the fault response combined with the range of values of the data volume imply that computer-based fault extraction techniques would perform very well with the spectral similarity attribute.

To investigate the validity of the features identified by spectral similarity, we extracted faults over a short time interval using a data range cutoff and enforcing a strict lower limit to the number of points clustered (via *k*-means clustering) to 10,000. We extracted 332 total fault planes, which were then checked for quality by a Ph.D. structural geologist with experience in this

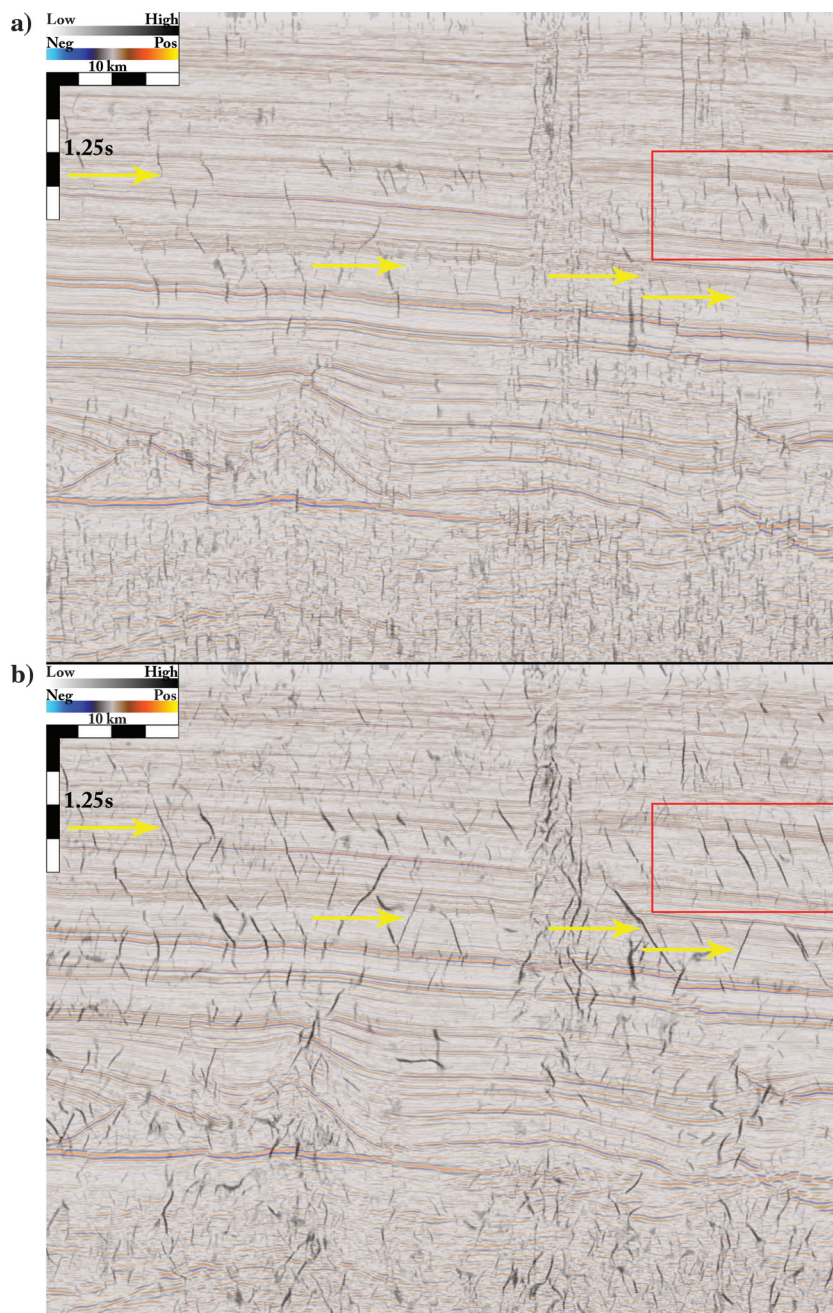


Figure 7. Corendered vertical section comparing the results from the (a) fault-enhanced similarity enhancement and (b) spectral similarity. The red rectangle highlights an area where the spectral similarity shows more accurate fault dip, and the yellow arrows indicate areas where the spectral similarity has increased the connectivity of the fault response.

basin. It was determined that 33% of the faults (108) required no editing, 63% of the faults (209) required only basic editing, and the remaining 4% (15) required editing of the 3D mesh (the software incorrectly connected the points). Moreover, “basic editing” consisted of splitting (dominantly in the vertical direction) the correctly placed points that were clustered together to make larger fault planes. These results are shown in Figure 9. Our initial constraints, specifically the number of points required per cluster, were overly conservative, as indicated from the number of readily identifiable faults left uninterpreted. These faults were, in fact, interpreted by

the computer, but their cluster sizes were below our 10,000-point lower bound. In the authors’ experience, the faults extracted from previous similarity attributes (and enhanced versions) require more significant editing, and the spectral similarity attribute greatly increases the efficiency of fault interpretation over traditional computer-based fault extraction workflows. In fault extraction comparisons, conducted by the same Ph.D. structural geologist, similar numbers of faults were interpreted by the computer, but the extracted surfaces were overly vertical and required significantly more complex and time-consuming point editing. Using an average

Figure 8. Time slice from the spectral similarity rendered with a crossline of seismic amplitude illustrating results of semimanual fault interpretation using commercial software. The yellow, blue, and purple points are interpreted fault planes.

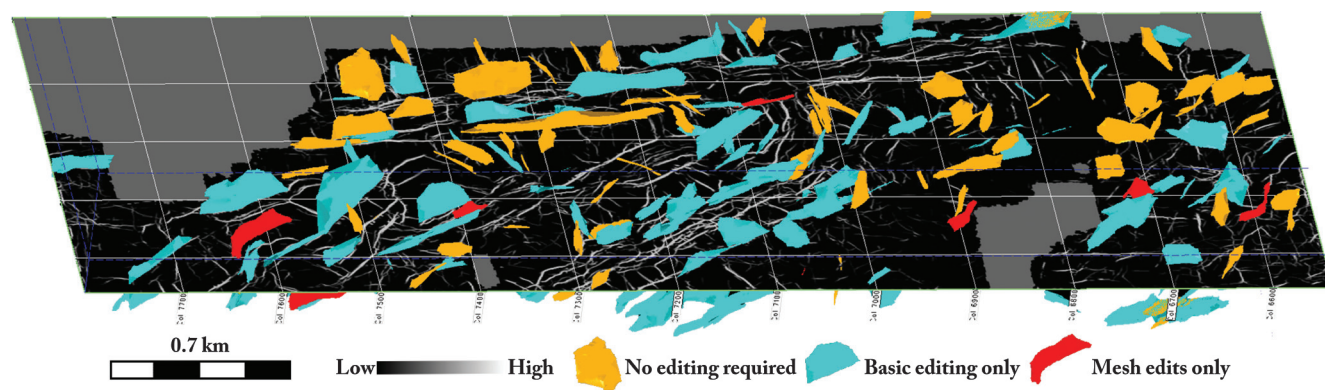


Figure 9. Computer-based fault interpretation using a minimum point population of 10,000 points per cluster rendered with the spectral similarity volume. The yellow faults require no edits, the blue faults require minor edits, and the red faults require interpolated mesh edits. The result was an increase in productivity of 6×–8× computer-based fault interpretations on other attribute volumes.

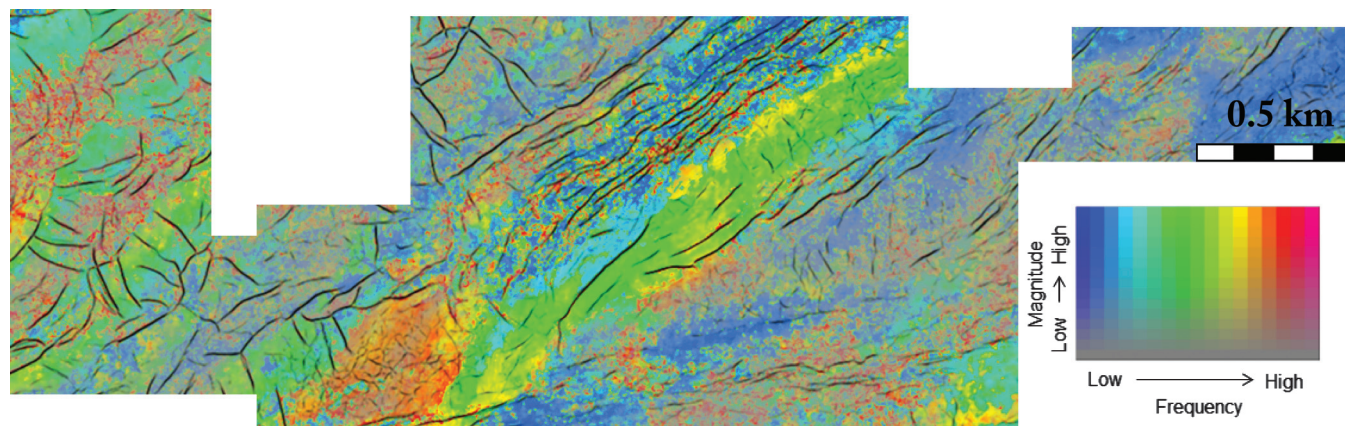


Figure 10. Corendered time slice of peak frequency and peak magnitude from CWT spectral decomposition with the spectral similarity volume. Peak frequency/magnitude provides an indication of lateral stratigraphic variation, and the spectral similarity provides structural information.

elapsed time over 20 fault edits from faults extracted on the spectral similarity attribute and commercially available similarity enhancements, we estimate an increase in human productivity of 6x–8x (the computation time is not accounted for).

In addition to fault surface interpretation, the spectral similarity attribute can provide a clear way to understand and communicate geologic complexity through multiattribute analysis and display. By combining this structural attribute with the peak frequency and peak magnitude from spectral decomposition, we can display the structural grain from the spectral similarity and the lateral lithologic variation as interpreted from the peak frequency and peak magnitude volumes (Figure 10). In this case, the low signal-to-noise zone in the lower center of the image is easily identifiable, while still displaying the major fault trends through this area. These faults were later confirmed through quality control and manual interpretation of the amplitude volume by basin experts. Many faults act as boundaries to the peak frequency, whereas other similar faults do not. This type of information may be beneficial to well planning and well placement in various reservoirs.

Case study no. 2: Low signal to noise

Similar to case study no. 1, the area for case study no. 2 is in an extensional regime, with normal faults striking approximately perpendicular to the extensional direction. Basement structures and salt movement have influenced the deposition and deformation patterns of the study area. Movement on a basement fault was accommodated by a series of faults oblique to the regional extension direction (Figures 11 and 12 rectangle). In addition, salt movement in the northeast area of the study

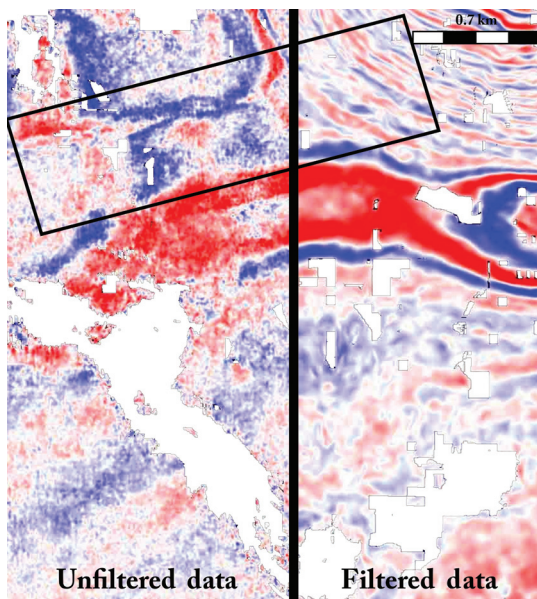


Figure 11. Time slice comparison of data prior to filtering and data after structure-orientated mean-/median-based filtering. The rectangle highlights a major fault zone in the data.

area created local variations from the regional stress regime that influenced fault orientations (Figure 11b, rectangle).

Customized workflow

In contrast to case study no. 1, this data set is heavily contaminated by noise (Figure 11, left side; the full supplementary figure can be accessed through the

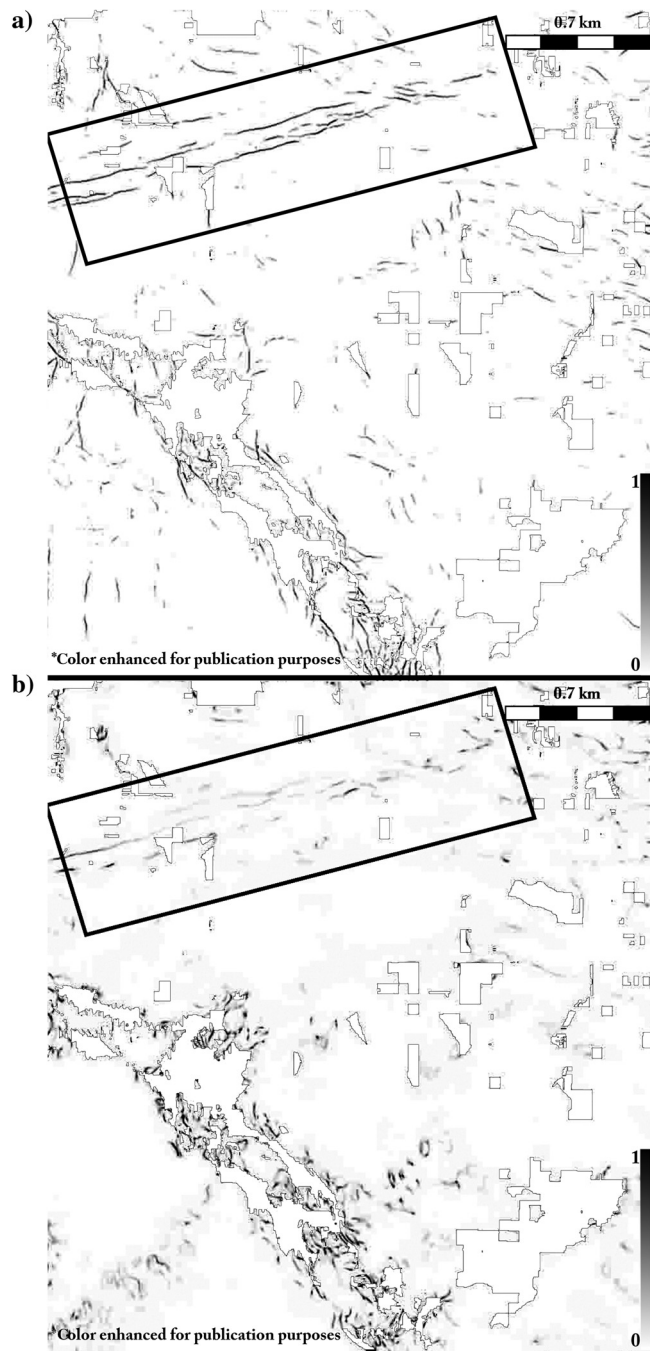


Figure 12. Time slice at the level of Figure 11 from (a) the spectral similarity volume and (b) a modified eigenstructure similarity. The fault zone highlighted by the rectangle is poorly resolved on the eigenstructure similarity, but it resolves into a trend of parallel faults on the spectral similarity.

following link: [s2.mpg](#)). Therefore, as a first step, we applied a series of progressively larger windowed, structurally orientated, and median/mean combination filters (Figure 11, right side). Small-scale fault identification is limited owing to heavy noise contamination, and noise reduction was paramount. Our filters began in a 3×3 window and were followed by 6×6 and 9×9 window filters. As in case study no. 1, we then used crosscorrelation-based spectral decomposition (Gao, 2013). Based on the visual inspection, we chose the 67 and 40 Hz volumes for our analysis. We also used the full-stack modified eigenstructure similarity (Garsztenkorn and Marfurt, 1999) for quality control. On each peak frequency volume, we computed a Sobel filter-based similarity (Al-Dossary and Al-Garni, 2013), which was followed by Pedersen et al. (2002)-style swarm intelligence and fault enhancement (Dorn et al., 2012). When calculating dip, we used a dip-scan method with a maximum of 60° and an increment of 2° (Marfurt, 2006). We then volumetrically summed these two volumes. The size of the original seismic is approximately 25 GB, and the total size of all intermediate products, parameter tests, software projects, duplicated data, and SEGY exports was 2.6 TB (63 GB of final products). The total time required for computation was approximately 29 h, and required intermittent human interaction (to initiate a process).

Results

The data set used in case study no. 2 is both contaminated by noise and heavily affected by poor acquisition coverage. This data set is of a lower fold and has an overall lower S/N than does case study no. 1. Nonetheless, spectral similarity greatly outperforms full-stack coherence and provides a clear indication of the complex fault systems present in the data (Figure 12; the full supplementary figure can be accessed through the following link: [s3.mpg](#)). Specifically, the rectangle from Figure 12 highlights a complex fault system whose existence is hinted at in the full-stack similarity, yet it is not fully resolved. Spectral similarity allows the interpreter to identify and interpret these systems more effectively.

Conclusions

Fault interpretation remains a time-consuming and tedious task that is punctuated by moments of complexity and difficulty. Edge-detection attributes are a critical tool in the interpreter's toolbox to assist with and increase efficiency of fault interpretation workflows. We have demonstrated that our new method of similarity enhancement, spectral similarity, greatly increases the vertical and horizontal response of discontinuities. Moreover, we believe that spectral similarity lends itself quite readily to computer-based fault extraction techniques, and we have shown the potential for a dramatic increase in productivity when using this technique as a basis for such extractions. These improvements are a direct result of the inclusion of spectral decomposition,

swarm intelligence, and orientated filtering into our workflow, which comes at a cost of computation time and scratch storage space. We provide for the use of curvature, total energy, or similarity style attributes combined into one fault detection volume. This enables the interpreter to identify which attributes highlight faults (or other linear features) optimally in their data set. Our spectral similarity workflow reduces or eliminates many algorithmic anomalies present in similarity attributes by estimating a more realistic fault dip, reducing noise, and removing stair-step discontinuities.

Acknowledgments

We would like to thank BHP Billiton and Global Geophysical Services Inc., for encouraging this work and for permission to present these results. We would also like to thank our colleagues at BHP Billiton who provided valuable suggestions and edits. We specifically would like to thank C. Docherty, who provided valuable assistance and several images used in this study.

References

- Al-Dossary, S., and K. Al-Garni, 2013, Fault detection and characterization using a 3D multidirectional Sobel filter: Presented at the Saudi Arabia Section Technical Symposium and Exhibition, SPE, SPE-168061-MS.
- Aqrabi, A., and T. Boe, 2011, Improved fault segmentation using a dip guided and modified 3D Sobel filter: 81st Annual International Meeting, SEG, Expanded Abstracts, 999–1003.
- Bahorich, M. S., and S. L. Farmer, 1995, 3-D seismic discontinuity for faults and stratigraphic features: The coherence cube: 65th Annual International Meeting, SEG, Expanded Abstracts, 93–96, doi: [10.1190/1.1887523](https://doi.org/10.1190/1.1887523).
- Basir, H., A. Javaherian, and M. Yaraki, 2013, Multi-attribute ant-tracking and neural network for fault detection: A case study of an Iranian oilfield: Journal of Geophysics and Engineering, **10**, 015009, doi: [10.1088/1742-2132/10/1/015009](https://doi.org/10.1088/1742-2132/10/1/015009).
- Dorn, G., B. Kadlec, and M. Patty, 2012, Imaging faults in 3D seismic volumes: 82nd Annual International Meeting, SEG, Expanded Abstracts, doi: [10.1190/segam2012-1538.1](https://doi.org/10.1190/segam2012-1538.1).
- Gao, D., 2013, Wavelet spectral probe for seismic structure interpretation and fracture characterization: A workflow with case studies: Geophysics, **78**, no. 5, O57–O67, doi: [10.1190/geo2012-0427.1](https://doi.org/10.1190/geo2012-0427.1).
- Garsztenkorn, A., and K. J. Marfurt, 1999, Eigenstructure-based coherence computations as an aid to 3-D structural and stratigraphic mapping: Geophysics, **64**, 1468–1479, doi: [10.1190/1.1444651](https://doi.org/10.1190/1.1444651).
- Marfurt, K. J., 2006, Robust estimates of reflector dip and azimuth: Geophysics, **71**, no. 4, P29–P40, doi: [10.1190/1.2213049](https://doi.org/10.1190/1.2213049).
- Marfurt, K. J., R. Kirlin, S. Farmer, and M. Bahorich, 1998, 3-D seismic attributes using a semblance-based coherency algorithm: Geophysics, **63**, 1150–1165, doi: [10.1190/1.1444415](https://doi.org/10.1190/1.1444415).

Pedersen, S. I., T. Randen, L. Sønneland, and O. Steen, 2002, Automatic 3D fault interpretation by artificial ants: 72nd Annual International Meeting, SEG, Expanded Abstracts, 512–515.

Randen, T., S. Pedersen, and L. Sønneland, 2001, Automatic extraction of fault surfaces from three-dimensional seismic data: 71st Annual International Meeting, SEG, Expanded Abstracts, 551–554.



Dustin T. Dewett received an M.S. (2013) in geophysics from the University of Oklahoma, studying the seismic character of Middle-Eastern carbonates near hydrocarbon reservoirs. After joining BHP Billiton in 2013, he became involved in quantitative seismic interpretation in conventional and unconventional reservoirs. He is a veteran of the U.S. Navy Submarine Force, and he is currently pursuing a Ph.D. in geophysics from the University

of Oklahoma. His research interests include the application of multiattribute analysis to structural and stratigraphic features and leveraging seismic attributes to increase the efficiency of the seismic interpreter.



Alissa A. Henza received a Ph.D. (2009) from Rutgers University, studying the fault patterns produced by multiple phases of noncoaxial extension. Before joining BHP Billiton, she co-led the AAPG/SEPM short course “Seismic Expression of Structural Styles: A Modeling Perspective” at the 2008 AAPG Annual Convention

and Exhibition. She also assisted with research projects funded by Husky Energy to investigate the development of fault patterns during multiple phases of extension in the Jeanne d'Arc Basin, Newfoundland, Canada. Her research interests include the effects of pre-existing fault patterns on newly forming faults and fractures, and developing techniques to aid in fault and fracture interpretation.